Supporting Information for

Determination of the Molecular Structures of Ferric Enterobactin and Ferric Enantioenterobactin using Racemic Crystallography

Timothy C. Johnstone[1] and Elizabeth M. Nolan[1,*]

[1] Department of Chemistry, Massachusetts Institute of Technology, 77 Massachusetts Avenue, Cambridge, MA 02139, USA

*Corresponding author: lnolan@mit.edu

Phone: 617-452-2495

Fax: 617-324-0505

This Supporting Information includes:

Methods

Materials. All chemicals were used as received from commercial suppliers. The metalation, salt metathesis, purification, and crystallization procedures were performed in a well-ventilated fume hood under atmospheric conditions with no measures taken to exclude oxygen or moisture. K_3[Fe(ent)], used for spectroscopic comparison, was prepared as previously described.[1]

Instrumentation. Optical absorption spectra were recorded at room temperature on an Agilent 8453 diode array UV-visible spectrophotometer using a 1-cm path length quartz cuvette. Circular dichroism (CD) spectra were recorded with an Olis RSM100 CD spectrometer and a cylindrical quartz cuvette with a path length of 0.1 cm, using an integration time of 1 s nm^{-1}. Three CD spectra were averaged for each sample. Mass spectrometry measurements were performed in both positive and negative ion modes by direct injection into an Agilent 6538 Q-TOF electrospray ionization mass spectrometer. Microanalysis for carbon, hydrogen, and nitrogen was performed on a Flash 2000 CHNS Analyzer. Single crystal X-ray diffraction was carried out on a Bruker APEX II diffractometer as described below.

Synthesis of $(AsPh_4)_3$[Fe(DL-ent)]. Enterobactin and enantioenterobactin were prepared as previously described, using the *N*-trityl-*O*-methyl esters of L-serine and D-serine, respectively.[2,3] Briefly, the esters were cyclotrimerized using 2,2-dibutyl-1,3,2-dioxastannolane to template the formation of the 12-membered ring. Following removal of the trityl protecting groups, each of the amine functionalities was coupled to a benzyl-protected 2,3-dihyroxybenzoic acid. Removal of the benzyl protecting groups by hydrogenation over Pd/C afforded the free ligands. A 1:1

mixture of enterobactin (28 mg, 42 μmol) and enantioenterobactin (28 mg, 42 μmol) was dissolved in methanol (6 mL). A solution of $Fe(acac)_3$ (30 mg, 85 μmol) in methanol (4 mL) was added to the ligand solution and the reaction mixture turned a deep violet color. A solution of potassium hydroxide (15 mg, 0.27 mmol) in methanol (4 mL) was added slowly and the color of the solution changed to a deep red. The solvent was then removed under reduced pressure. Dichloromethane (8 mL) was added to the residue, which did not dissolve. A solution containing a two-fold excess of tetraphenylarsonium chloride (225 mg, 0.54 mmol) in dichloromethane (5 mL) was added and the residue subsequently dissolved. The deep red solution was filtered through a pad of Celite and pentane was added to precipitate a red solid. Pentane was added until the red color was fully discharged from the supernatant. The deep red solid was collected by filtration on a glass frit and washed with water (40 mL). The solid was dried under vacuum. Yield: 146 mg, 93%. CD spectroscopy (DMF): silent. HRMS (ESI-QTOF): positive mode *m*/*z* $[M]^+$ calc'd for $C_{24}H_{20}As^+$ 383.0775 Da, measured 383.0779 Da; negative mode *m*/*z* $[M+2H^+]^-$ calc'd for $C_{30}H_{23}FeN_3O_{15}^-$ 721.0484 Da, measured 721.0494 Da. Elemental analysis for $C_{102}H_{81}As_3FeN_3O_{15}$ calculated (found): C 65.54 (65.92), H 4.37 (4.51), N 2.25 (2.01).

Crystallography. Preliminary attempts at crystallization using alcoholic solvents and water or diethyl ether as precipitants were unsuccessful, resulting only in the deposition of red films or oils. Initial hits were obtained with halocarbon solutions of $(AsPh_4)_3$[Fe(DL-ent)] and alkanes as precipitants. For instance, vapor diffusion of pentane into either *o*-dichlorobenzene or 1,2-dichloroethane solutions of the salt and layering pentane onto a dichloromethane solution of the salt afforded deep red plates. These plates were consistently too thin for X-ray diffraction analysis. Ultimately, crystals of $(AsPh_4)_3$[Fe(DL-ent)]·6DMF·H_2O were grown by placing a 0.5

mL DMF solution of the compound in a 4-mL glass vial, sealing the vial with aluminum foil, piercing the foil once with a 20-gauge needle, and placing it in a 20-mL vial containing diethyl ether (7 mL). The 20-mL vial was capped and the assembly was placed in a -20 °C freezer. The crystals formed over the course of two months. The crystals repeatedly redissolved during attempts to remove them from the mother liquor, so the mother liquor was diluted 5-fold with diethyl ether and allowed to equilibrate at -20 °C for one day. This procedure was repeated twice to achieve a net 125-fold dilution. Crystals were readily removed from this mother liquor without loss of structure.

The crystals were coated in Paratone-N oil and examined under a microscope. A suitable crystal was selected, mounted on Bruker APEX II diffractometer using a MiTeGen loop (Figure S1), and cooled to 150 K under a stream of nitrogen using an Oxford CryoSystems cryostream. The sample was irradiated with Mo Kα radiation. The data were collected and processed using the *APEXII* software.[4] Data reduction was performed with *SAINT* and an absorption correction was applied using *SADABS*.[5-7] The space group type was assigned based on the systematically absent reflections using *XPREP* and the initial solution was obtained using intrinsic phasing with *SHELXT*.[8,9] This initial solution was refined using standard techniques using *SHELXL*.[10,1112] All non-hydrogen atoms were refined anisotropically. Carbon-bound hydrogen atoms were placed at calculated positions and refined using a riding model with coupled thermal parameters. The U_{iso} of each hydrogen atom was set equal to 1.2 times the equivalent isotropic displacement parameter of the atom to which it was attached. A factor of 1.5 was used for the methyl groups of the DMF molecule. The amide hydrogen atoms were treated similarly, but the riding model was relaxed to allow the N–H distance to refine. The three N–H distances were restrained to have similar values. The hydrogen atoms on the water of crystallization could not be located in the

difference Fourier maps and so were not included in the model. The bond lengths and angles of the three $AsPh_4^+$ cations were also restrained to be similar. Finally, similarity and rigid bond restraints were placed on the thermal parameters of all atoms in the structure.

During refinement, disordered electron density centered on two crystallographically distinct inversion centers within the unit cell could not be successfully modeled. The void volumes and electron counts are consistent with the presence of 10 unassigned DMF molecules in each void (5 unidentified DMF molecules in the asymmetric unit, Figure S7). This assignment is consistent with the measured density of the crystal. The density of the crystals was assessed by isopycnic flotation in a mixture of hexane and 1,6-dibromohexane. The ratio of solvents was adjusted until the crystals suspended in this mixture neither rose nor sank for 3 h following agitation (Figure S4). The formula weight for $(AsPh_4)_3[Fe(\text{DL-ent})]\cdot 6DMF\cdot H_2O$ (2325.97 Da) and $Z = 4$, afford a unit cell weight of 9303.88 Da (1.545×10^{-23} kg). In conjunction with a unit cell volume of 1.025 m^3, this unit cell weight affords a calculated density of 1.51 g/mL. The average of three isopycnic flotation measurements afforded a measured density of 1.50(3) g/mL. The effects of the disordered solvent were masked using *SQUEEZE*.[13] The final model was validated and checked for missed symmetry and possible twinning with *PLATON*.[14,15] The crystallographic parameters for the final model are collected in Table S1. Selected bond lengths and angles for the $[Fe(\text{DL-ent})]^{3-}$ complex anion are collected in Table S2. Hydrogen bond lengths and angles are collected in Table S3.

Computational Studies. Electronic structure calculations were performed with *ORCA* using spin unrestricted density functional theory (DFT) at the PBE0/def2-TZVPP level of theory.[16] The resolution of the identity approximation was used throughout.[17,18] The iron center was treated as

high-spin Fe(III) and the spin multiplicity of the complex was accordingly set to 6. The structure of the $[Fe(ent)]^{3-}$ anion was optimized in the gas phase (Table S4) and a frequency calculation confirmed, through the absence of imaginary frequencies, that the optimized structure lies at a minimum on its potential energy surface. The electron density obtained at this geometry was used in a topological (AIM) analysis conducted with the *MultiWFN* program.[19] The influence of hydrogen-bonding from second coordination sphere water on the structure of $[Fe(ent)]^{3-}$ was investigated by explicitly including a water molecule within hydrogen bonding distance of one of the *meta* catecholate oxygen atoms and reoptimizing the structure (Table S5). Coordinates for $[Fe(D\text{-ent})]^{3-}$ were obtained by inverting the optimized structure of $[Fe(ent)]^{3-}$, i.e. via application of the matrix (-1 0 0 0 -1 0 0 0 -1).

Protein docking studies were carried out with *AutoDock Vina* using the crystallographically determined coordinates of $[Fe(ent)]^{3-}$ or $[Fe(D\text{-ent})]^{3-}$ for the ligand.[20] The charges on the atoms were set to the Mulliken charges obtained from the electronic structure calculations described above. Carbon-bound hydrogen atoms were deleted and the charge of the carbon was taken as the sum of the charges on the carbon and the bound hydrogen atoms. The crystallographically-determined coordinates of Scn (PDB: 1L6M)[21] or FeuA (PDB: 2XUZ)[22] were used for the protein, following deletion of any small molecule ligands and addition of polar hydrogen atoms. Both the protein and the iron complex were treated as rigid bodies. The binding affinities obtained from the docking studies are collected in Table S6.

Methods References

(1) Abergel, R. J.; Warner, J. A.; Shuh, D. K.; Raymond, K. N. *J. Am. Chem. Soc.* **2006**, *128*, 8920.

(2) Ramirez, R. J. A.; Karamanukyan, L.; Ortiz, S.; Gutierrez, C. G. *Tetrahedron Lett.* **1997**, *38*, 749.

(3) Zheng, T.; Bullock, J. L.; Nolan, E. M. *J. Am. Chem. Soc.* **2012**, *134*, 18388.

(4) Bruker, *APEX2*, **2008**, Madison, Wisconsin.

(5) Bruker, *SAINT: SAX Area-Detector Integration Program*, **2008**, Madison, Wisconsin.

(6) Bruker, *SADABS: Area-Detector Absorption Correction*, **2001**, Madison, Wisconsin.

(7) Krause, L.; Herbst-Irmer, R.; Sheldrick, G. M.; Stalke, D. *J. Appl. Crystallogr.* **2015**, *48*, 3.

(8) Bruker, *XPREP*, **2008**, Madison, Wisconsin.

(9) Sheldrick, G. M. *Acta Crystallogr. Sect. A* **2015**, *71*, 3.

(10) Müller, P. *Crystallogr. Rev.* **2009**, *15*, 57.

(11) Müller, P. *Crystal Structure Refinement: A Crystallographer's Guide to SHELXL*; Oxford University Press: Oxford ; New York, 2006.

(12) Sheldrick, G. M. *Acta Crystallogr. Sect. C* **2015**, *71*, 3.

(13) Spek, A. L. *Acta Crystallogr. Sect. C* **2015**, *71*, 9.

(14) Spek, A. L. *J. Appl. Crystallogr.* **2003**, *36*, 7.

(15) Spek, A. L. *Acta Crystallogr. Sect. D* **2009**, *65*, 148.

(16) Neese, F. *Wiley Interdiscip. Rev.: Comput. Mol. Sci.* **2012**, *2*, 73.

(17) Neese, F. *J. Comput. Chem.* **2003**, *24*, 1740.

(18) Neese, F.; Wennmohs, F.; Hansen, A.; Becker, U. *Chem. Phys.* **2009**, *356*, 98.

(19) Lu, T.; Chen, F. *J. Comput. Chem.* **2012**, *33*, 580.

(20) Trott, O.; Olson, A. J. *J. Comput. Chem.* **2010**, *31*, 455.

(21) Goetz, D. H.; Holmes, M. A.; Borregaard, N.; Bluhm, M. E.; Raymond, K. N.; Strong, R. K. *Mol. Cell* **2002**, *10*, 1033.

(22) Peuckert, F.; Ramos-Vega, A. L.; Miethke, M.; Schwörer, C. J.; Albrecht, A. G.; Oberthür, M.; Marahiel, M. A. *Chem. Biol.* **2011**, *18*, 907.

Table S1. Crystallographic information for $(AsPh_4)_3[Fe(DL\text{-ent})]\cdot H_2O\cdot 6DMF$.

Empirical formula[a]	$C_{120}H_{123}As_3FeN_9O_{22}$ ($C_{105}H_{88}As_3FeN_4O_{17}$)
Formula weight[a]	2325.97 (1958.40)
Temperature (K)	150(2)
Wavelength (Å)	0.71073
Crystal system	Monoclinic
Space group type	$P2_1/n$
a (Å)	23.005(5)
b (Å)	14.524(3)
c (Å)	30.713(8)
β (°)	92.742(9)
Volume (Å^3)	10250(4)
Z	4
Crystal size (mm^3)	0.18 × 0.14 × 0.08
Calculated density (Mg m^{-3})[a]	1.51 (1.27)
Measured density (Mg m^{-3})	1.50(3)
θ range (°)	1.55 to 21.26
Reflections collected	96008
Independent reflections	11403
Parameters	1174
Completeness	99.9%
R_{int}	25.8%
R_{sigma}	16.5%
R_1 (I > 2σ)[b]	9.74%
R_1 (all data)[b]	22.3%
wR_2 (I > 2σ)[c]	18.6%
wR_2 (all data)[c]	26.8%
Goodness of fit, S[d]	1.031

[a] The initial values provided correspond to those for $(AsPh_4)_3[Fe(DL\text{-ent})]\cdot H_2O\cdot 6DMF$ and the values in parentheses correspond those obtained only using atoms included in the final model.
[b] $R_1 = \Sigma[|F_o|-|F_c|]/\Sigma[|F_o|]$
[c] $wR_2 = \{\Sigma[w(F_o^2 - F_c^2)^2]/\Sigma[w(F_o^2)]\}^{0.5}$; where $w = 1/[\sigma^2(F_o^2) + (0.0825P)^2 + 106.75P]$; $P = [\max(F_o^2, 0)+2F_c^2]/3$
[d] $S = \{\Sigma[w(F_o^2 - F_c^2)^2]/(r-p)]\}^{0.5}$; where r is the number of independent reflections and p is the number of refined parameters

Table S2. Selected bond lengths (Å), bond angles (°), and torsion angles (°) for the complex anion of $(AsPh_4)_3[Fe(DL\text{-ent})]\cdot H_2O\cdot 6DMF$. Values are provided for the entire primary coordination sphere, but otherwise only for one third of the complex; a full listing is available in the corresponding CIF. A legend for atom labels is provided below (Page S12).

Fe(1)-O(1A)	2.032(9)	O(2C)-Fe(1)-O(2B)	94.2(4)	Fe(1)-O(1A)-C(1A)-C(6A)	-176.0(10)
Fe(1)-O(1B)	2.036(10)	O(2C)-Fe(1)-O(2A)	92.6(4)	Fe(1)-O(1A)-C(1A)-C(2A)	6.3(15)
Fe(1)-O(1C)	2.040(9)	O(2B)-Fe(1)-O(2A)	90.1(4)	Fe(1)-O(2A)-C(2A)-C(3A)	178.7(11)
Fe(1)-O(2A)	2.019(10)	O(2C)-Fe(1)-O(1A)	160.7(4)	Fe(1)-O(2A)-C(2A)-C(1A)	1.9(16)
Fe(1)-O(2B)	2.007(9)	O(2B)-Fe(1)-O(1A)	103.4(4)	O(1A)-C(1A)-C(2A)-O(2A)	-5.5(19)
Fe(1)-O(2C)	1.966(9)	O(2A)-Fe(1)-O(1A)	79.7(4)	C(6A)-C(1A)-C(2A)-O(2A)	176.7(12)
O(1A)-C(1A)	1.336(16)	O(2C)-Fe(1)-O(1B)	106.2(4)	O(1A)-C(1A)-C(2A)-C(3A)	177.5(12)
O(2A)-C(2A)	1.324(17)	O(2B)-Fe(1)-O(1B)	79.7(4)	C(6A)-C(1A)-C(2A)-C(3A)	0(2)
O(3A)-C(7A)	1.251(17)	O(2A)-Fe(1)-O(1B)	159.1(4)	O(2A)-C(2A)-C(3A)-C(4A)	-179.0(13)
O(4A)-C(10B)	1.324(19)	O(1A)-Fe(1)-O(1B)	85.0(4)	C(1A)-C(2A)-C(3A)-C(4A)	-2(2)
O(4A)-C(9A)	1.462(17)	O(2C)-Fe(1)-O(1C)	79.7(4)	C(2A)-C(3A)-C(4A)-C(5A)	4(2)
O(5A)-C(10A)	1.187(18)	O(2B)-Fe(1)-O(1C)	161.8(4)	C(3A)-C(4A)-C(5A)-C(6A)	-3(2)
N(1A)-C(7A)	1.359(19)	O(2A)-Fe(1)-O(1C)	107.2(4)	O(1A)-C(1A)-C(6A)-C(5A)	-176.5(12)
N(1A)-C(8A)	1.417(19)	O(1A)-Fe(1)-O(1C)	85.6(4)	C(2A)-C(1A)-C(6A)-C(5A)	1(2)
N(1A)-H(1A)	0.85(8)	O(1B)-Fe(1)-O(1C)	85.5(4)	O(1A)-C(1A)-C(6A)-C(7A)	12(2)
C(1A)-C(6A)	1.399(19)	C(1A)-O(1A)-Fe(1)	113.2(9)	C(2A)-C(1A)-C(6A)-C(7A)	-170.0(13)
C(1A)-C(2A)	1.40(2)	C(2A)-O(2A)-Fe(1)	113.7(10)	C(4A)-C(5A)-C(6A)-C(1A)	1(2)
C(2A)-C(3A)	1.40(2)	C(10B)-O(4A)-C(9A)	114.0(13)	C(4A)-C(5A)-C(6A)-C(7A)	172.1(13)
C(3A)-C(4A)	1.39(2)	C(7A)-N(1A)-C(8A)	123.0(14)	C(8A)-N(1A)-C(7A)-O(3A)	-9(2)
C(4A)-C(5A)	1.38(2)	C(7A)-N(1A)-H(1A)	118.5	C(8A)-N(1A)-C(7A)-C(6A)	172.5(13)
C(5A)-C(6A)	1.417(19)	C(8A)-N(1A)-H(1A)	118.5	C(1A)-C(6A)-C(7A)-O(3A)	180.0(13)
C(6A)-C(7A)	1.44(2)	O(1A)-C(1A)-C(6A)	123.2(14)	C(5A)-C(6A)-C(7A)-O(3A)	9(2)
C(8A)-C(10A)	1.50(2)	O(1A)-C(1A)-C(2A)	116.0(13)	C(1A)-C(6A)-C(7A)-N(1A)	-2(2)
C(8A)-C(9A)	1.52(2)	C(6A)-C(1A)-C(2A)	120.7(14)	C(5A)-C(6A)-C(7A)-N(1A)	-173.3(12)
C(10A)-O(4C)	1.352(18)	O(2A)-C(2A)-C(3A)	123.3(15)	C(7A)-N(1A)-C(8A)-C(10A)	-99.6(16)
		O(2A)-C(2A)-C(1A)	117.0(14)	C(7A)-N(1A)-C(8A)-C(9A)	129.1(14)
		C(3A)-C(2A)-C(1A)	119.6(15)	C(10B)-O(4A)-C(9A)-C(8A)	93.8(16)
		C(4A)-C(3A)-C(2A)	118.8(16)	N(1A)-C(8A)-C(9A)-O(4A)	59.0(17)
		C(4A)-C(3A)-H(3A)	120.6	C(10A)-C(8A)-C(9A)-O(4A)	-73.2(18)
		C(2A)-C(3A)-H(3A)	120.6	N(1A)-C(8A)-C(10A)-O(5A)	142.7(18)
		C(5A)-C(4A)-C(3A)	123.0(15)	C(9A)-C(8A)-C(10A)-O(5A)	-85(2)
		C(5A)-C(4A)-H(4A)	118.5	N(1A)-C(8A)-C(10A)-O(4C)	-40.4(19)
		C(3A)-C(4A)-H(4A)	118.5	C(9A)-C(8A)-C(10A)-O(4C)	91.6(17)
		C(4A)-C(5A)-C(6A)	118.3(15)	Fe(1)-O(1A)-C(1A)-C(6A)	-176.0(10)
		C(4A)-C(5A)-H(5A)	120.8		
		C(6A)-C(5A)-H(5A)	120.8		
		C(1A)-C(6A)-C(5A)	119.4(15)		
		C(1A)-C(6A)-C(7A)	122.3(14)		
		C(5A)-C(6A)-C(7A)	117.7(14)		
		O(3A)-C(7A)-N(1A)	119.7(16)		
		O(3A)-C(7A)-C(6A)	123.0(15)		
		N(1A)-C(7A)-C(6A)	117.3(14)		
		N(1A)-C(8A)-C(10A)	114.3(13)		
		N(1A)-C(8A)-C(9A)	113.9(13)		
		C(10A)-C(8A)-C(9A)	112.6(14)		
		N(1A)-C(8A)-H(8A)	104.9		

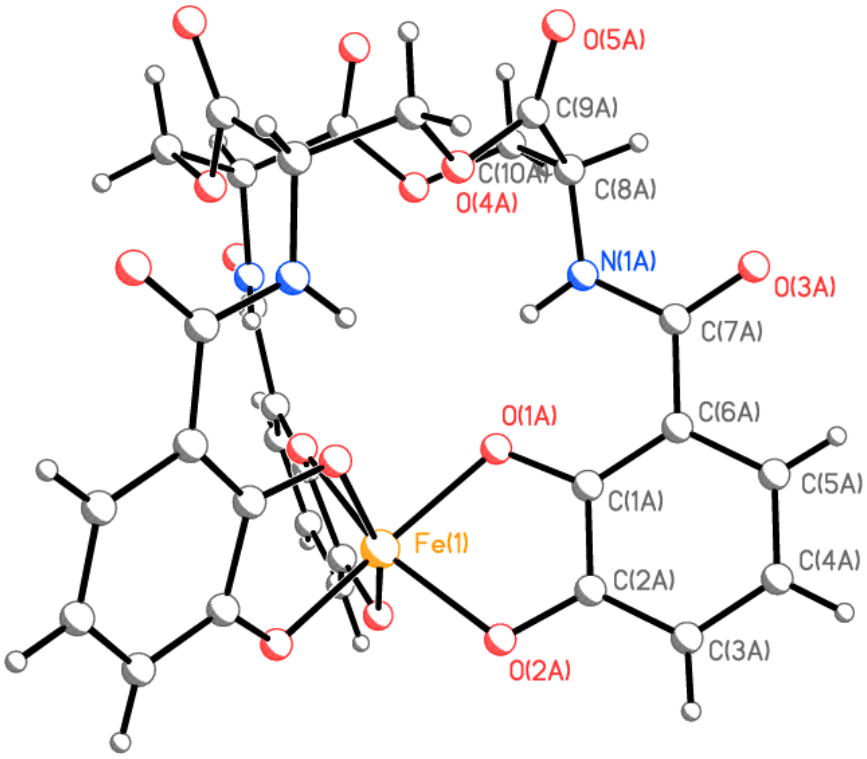
O(5A)
C(9A)
C(10A)
O(4A)
C(8A)
N(1A)
O(3A)
C(7A)
C(6A)
O(1A)
C(1A)
C(5A)
Fe(1)
C(2A)
C(4A)
C(3A)
O(2A)

Table S3. Hydrogen bond lengths (Å) and angles (°) for $(AsPh_4)_3[Fe(DL\text{-}ent)]\cdot H_2O\cdot 6DMF$.

D-H···A	d(D-H)	d(H···A)	d(D···A)	∠(DHA)
N(1A)-H(1A)···O(1A)	0.85(8)	1.87	2.571(16)	138.7
N(1B)-H(1B)···O(1B)	0.86(8)	1.89	2.582(16)	137.2
N(1C)-H(1C)···O(1C)	0.85(8)	2.01	2.639(16)	129.3

Table S4. Cartesian coordinates (Å) for the optimized structure of spin 5/2 $[Fe(ent)]^{3-}$.

Fe	0.624296	1.242668	4.167818
O	-0.509933	0.562194	2.549116
O	0.949030	-0.804461	4.475598
O	-1.128088	0.886687	5.215372
O	0.397925	2.906422	3.075868
O	2.555266	1.038808	3.704494
O	0.917101	2.282253	5.874172
O	-3.361799	-0.065196	-0.471331
O	2.013818	-4.860904	4.395939
O	-4.470361	0.480005	7.696304
O	-5.045483	-2.995951	2.221082
O	-2.027706	-5.503337	3.126209
O	-4.269907	-3.770800	6.319071
N	-2.237632	-0.933637	1.299161
N	0.365527	-3.326045	4.684428
N	-3.278004	-0.354697	5.955832
C	-0.884507	1.496645	1.730896
C	2.142820	-1.206536	4.172313
C	-1.250906	1.555505	6.318725
C	-0.331439	2.803301	2.002694
C	3.055488	-0.160804	3.773351
C	-0.112998	2.374522	6.665330
C	-0.617641	3.841714	1.126826
C	4.371848	-0.498324	3.490019
C	-0.196469	3.174635	7.799209
C	-1.477574	3.647540	0.028953
C	4.802942	-1.837898	3.543757
C	-1.355711	3.174415	8.599016
C	-2.056938	2.422799	-0.197391
C	3.924778	-2.842336	3.871504
C	-2.420251	2.360284	8.295954
C	-1.784932	1.331307	0.656512
C	2.578684	-2.549036	4.182264
C	-2.375061	1.510114	7.168139
C	-2.522709	0.077763	0.426301
C	1.663221	-3.674615	4.429768
C	-3.466245	0.536495	6.975292
C	-3.000834	-2.133022	1.292164
C	-0.652882	-4.317410	4.698424
C	-4.180365	-1.434653	5.758824
C	-4.124594	-2.221462	2.327169
C	-1.445766	-4.481077	3.399884
C	-3.595387	-2.827177	5.982446
C	-2.150222	-3.390216	1.411159
C	-1.639243	-4.156334	5.844122
C	-4.897914	-1.401316	4.413465
H	-0.177779	4.814567	1.328878
H	5.052718	0.296920	3.199571
H	0.656949	3.795083	8.058002
H	-1.698425	4.481601	-0.633242
H	5.835870	-2.076937	3.301849
H	-1.401288	3.820152	9.472090
H	-2.752536	2.261168	-1.011871
H	4.226462	-3.883417	3.886311
H	-3.307128	2.326276	8.917616
H	-1.569011	-0.692432	2.044271
H	0.168517	-2.315320	4.633629
H	-2.442205	-0.195807	5.376862
H	-3.512139	-2.178628	0.325257
H	-0.156058	-5.282070	4.835695
H	-4.959039	-1.329282	6.519851
H	-2.768341	-4.285682	1.352591
H	-1.403397	-3.389235	0.615506
H	-2.389385	-4.946449	5.829113
H	-1.095083	-4.176505	6.790136
H	-5.563547	-2.257653	4.303221
H	-5.465851	-0.471962	4.346971
O	-2.290492	-2.888511	5.734314
O	-3.949500	-1.389301	3.345322
O	-1.439554	-3.382105	2.651737

Table S5. Cartesian coordinates (Å) for the optimized structure of spin 5/2 $[Fe(ent)]^{3-}\cdot H_2O$.

Fe	0.570028	1.291667	4.193254
O	-0.565255	0.614410	2.580777
O	0.899517	-0.750331	4.504643
O	-1.177799	0.927086	5.232646
O	0.383567	2.961045	3.035399
O	2.498753	1.105315	3.739118
O	0.866008	2.321000	5.892267
O	-3.395123	-0.043794	-0.460330
O	2.019344	-4.795990	4.411620
O	-4.427427	0.345709	7.806584
O	-5.063748	-2.994521	2.230506
O	-2.004571	-5.490304	3.085121
O	-4.296304	-3.813394	6.260472
N	-2.277968	-0.901653	1.318422
N	0.343826	-3.290061	4.683002
N	-3.295148	-0.388049	5.983474
C	-0.915760	1.530969	1.731237
C	2.103419	-1.139832	4.219137
C	-1.274910	1.537499	6.372639
C	-0.342733	2.828573	1.941623
C	3.012675	-0.088260	3.832818
C	-0.141778	2.355740	6.723400
C	-0.556145	3.833752	1.015328
C	4.339987	-0.405904	3.586558
C	-0.194820	3.089969	7.901427
C	-1.412619	3.622106	-0.078962
C	4.787910	-1.738195	3.655841
C	-1.320226	3.020095	8.743761
C	-2.036407	2.410254	-0.249406
C	3.911950	-2.752496	3.957213
C	-2.381689	2.204410	8.433366
C	-1.807727	1.349997	0.649875
C	2.555416	-2.476325	4.233676
C	-2.366873	1.425452	7.256554
C	-2.555767	0.100266	0.435548
C	1.650965	-3.616064	4.450759
C	-3.453128	0.449579	7.052338
C	-3.031423	-2.107375	1.301004
C	-0.655113	-4.302018	4.675010
C	-4.199793	-1.463694	5.768243
C	-4.150183	-2.212245	2.337856
C	-1.439129	-4.462653	3.371608
C	-3.617600	-2.861319	5.959883
C	-2.168026	-3.356953	1.401026
C	-1.650334	-4.177267	5.817523
C	-4.924783	-1.403243	4.428607
H	-0.068668	4.791505	1.166332
H	5.017294	0.398614	3.314289
H	0.655660	3.712554	8.162093
H	-1.588693	4.430420	-0.783614
H	5.830393	-1.963890	3.445777
H	-1.341452	3.609897	9.656506
H	-2.727582	2.233310	-1.064367
H	4.224994	-3.789829	3.979027
H	-3.241868	2.113609	9.086049
H	-1.613728	-0.660471	2.065189
H	0.127973	-2.284896	4.642034
H	-2.479708	-0.201141	5.388082
H	-3.543739	-2.145998	0.334525
H	-0.139236	-5.257962	4.800391
H	-4.972129	-1.374780	6.537630
H	-2.776476	-4.258310	1.334624
H	-1.425618	-3.338363	0.601345
H	-2.392619	-4.974195	5.779844
H	-1.113076	-4.211863	6.766971
H	-5.594192	-2.255215	4.307877
H	-5.488336	-0.470410	4.377904
O	-2.309444	-2.912792	5.728169
O	-3.979741	-1.380833	3.357404
O	-1.452876	-3.353305	2.638563
O	1.824283	5.303094	3.058412
H	2.620027	4.883766	3.392545
H	1.248503	4.493133	3.064837

Table S6. Protein docking binding affinities of $[Fe(ent)]^{3-}$ and $[Fe(D\text{-}ent)]^{3-}$ for Scn and FeuA.

	Affinity (kcal mol^{-1})[a]
Scn	
$[Fe(ent)]^{3-}$	-9.2
$[Fe(D\text{-}ent)]^{3-}$	-11.7
FeuA	
$[Fe(ent)]^{3-}$	–
$[Fe(D\text{-}ent)]^{3-}$	-11.9

[a] The standard error of the affinities predicted by *Autodock Vina* is approximately 2.8 kcal/mol.[20]

Figure S1. Photograph of the single crystal of $(AsPh_4)_3[Fe(DL\text{-ent})]\cdot H_2O\cdot 6DMF$ from which the diffraction data were collected. Inset is a diagrammatic depiction with indexed crystal faces.

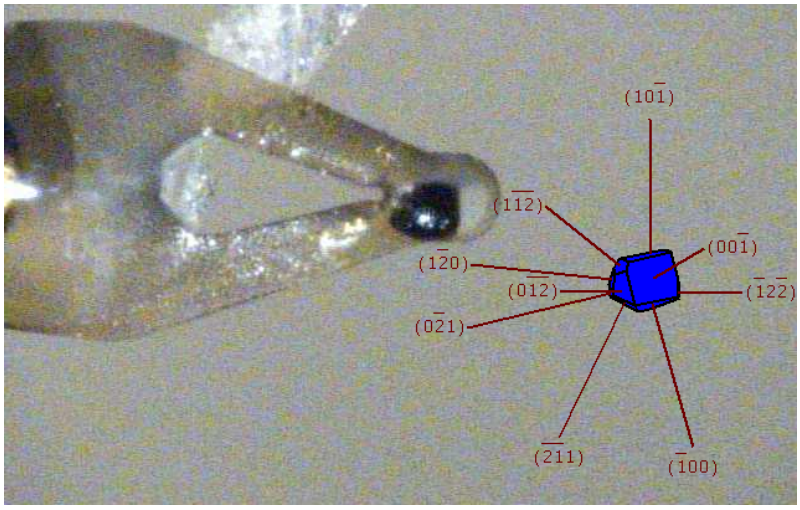

Figure S2. Thermal ellipsoid plot (50% probability level, hydrogen atoms shown as spheres of arbitrary radius) of the assigned contents of the asymmetric unit of $(AsPh_4)_3$[Fe(DL-ent)]·H_2O·6DMF. Color code: Fe orange, O red, N blue, C grey, As, green, H white.

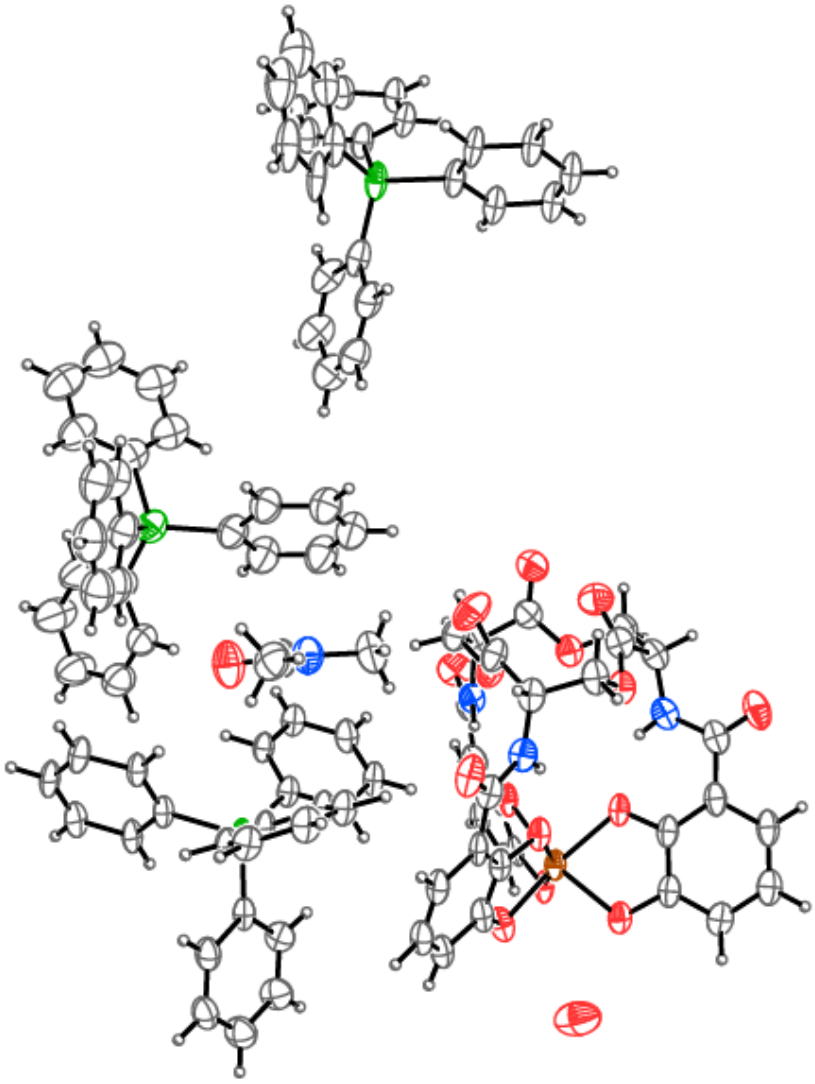

Figure S3. Intermolecular π-interactions in the crystal structure of $(AsPh_4)_3$[Fe(DL-ent)]·H_2O·6DMF. Molecules are depicted as balls joined by sticks and π-interactions are depicted with dashed lines. Color code: Fe orange, O red, N blue, C grey, As, green, H white.

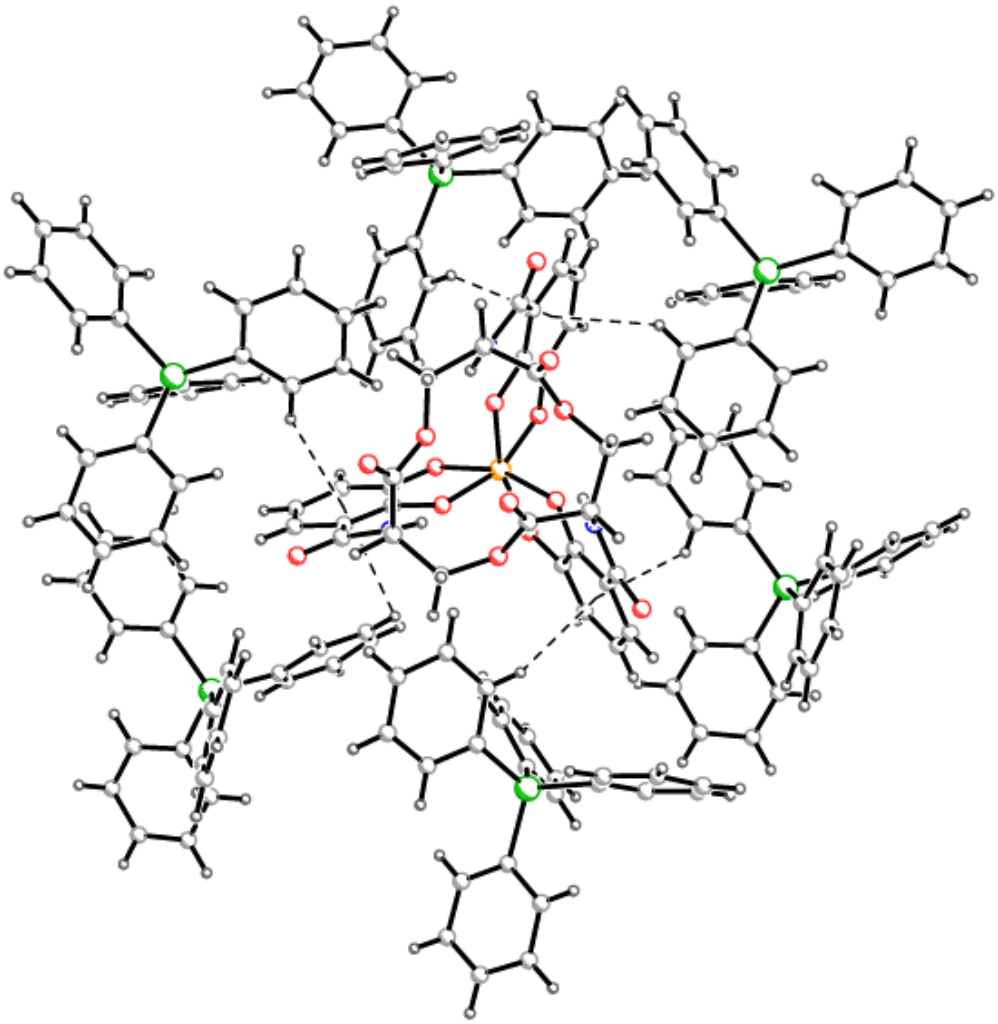

Figure S4. Photograph of crystals of $(AsPh_4)_3[Fe(DL\text{-ent})]\cdot H_2O\cdot 6DMF$ suspended in a mixture of hexane and 1,6-dibromohexane during density determination using isopycnic flotation.

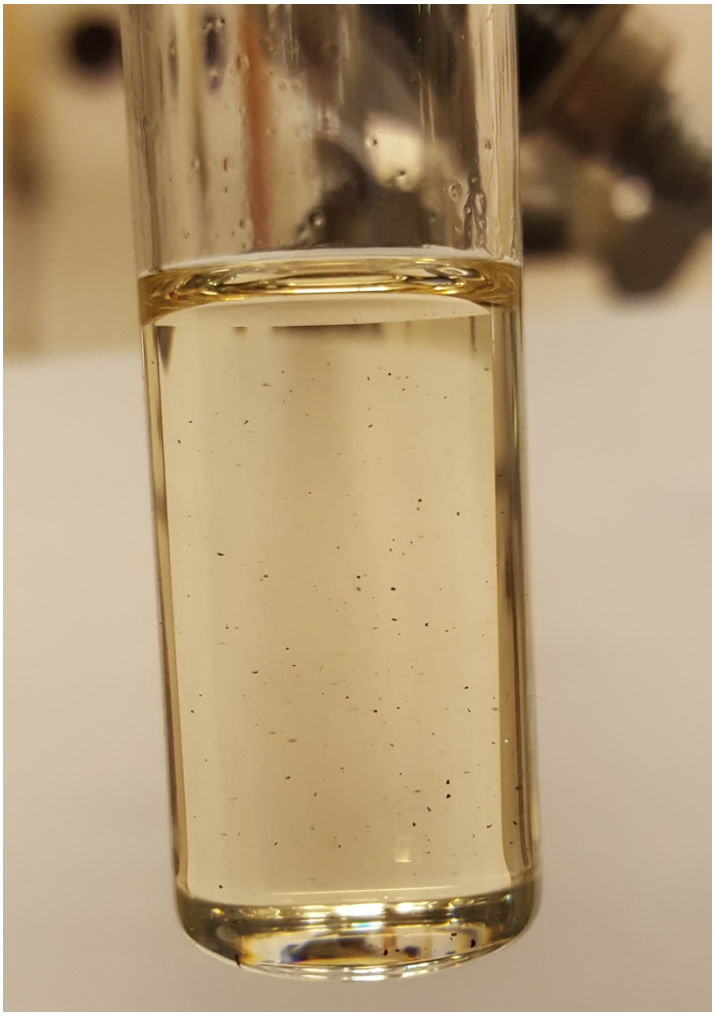

Figure S5. Packing diagram of $(AsPh_4)_3[Fe(DL\text{-ent})]\cdot H_2O\cdot 6DMF$, with molecules depicted as balls and sticks, viewed along the crystallographic *c* axis. Color code: Fe orange, O red, N blue, C grey, As, green, H white.

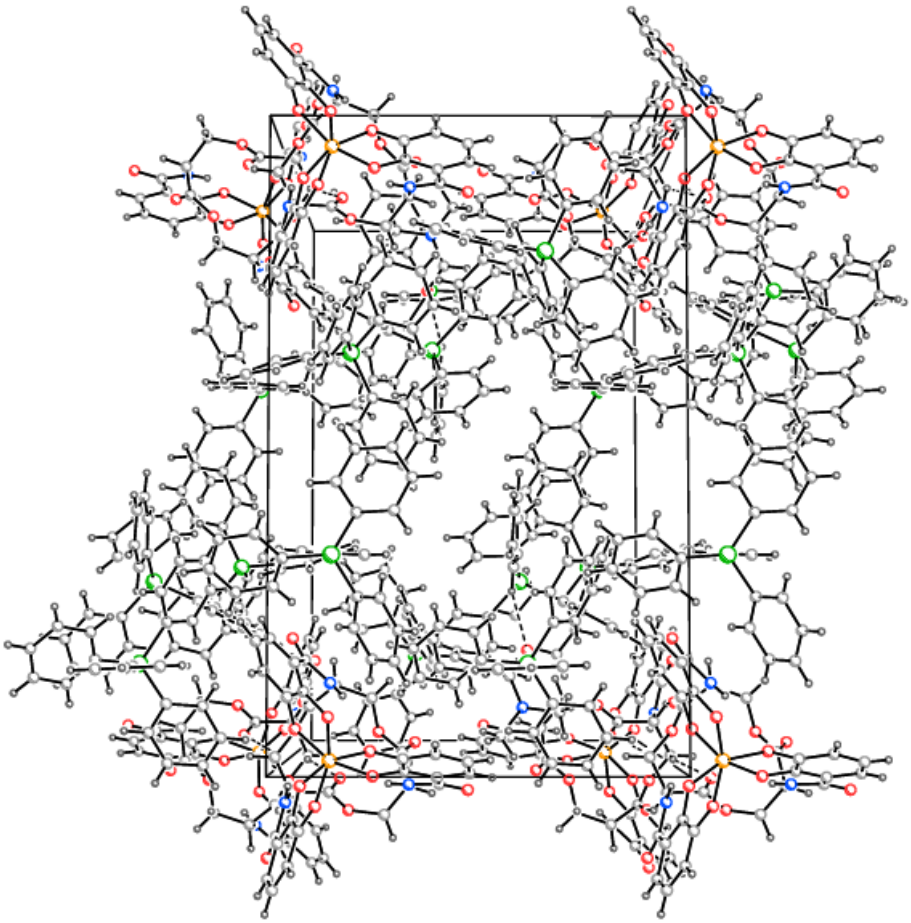

Figure S6. Coordination polyhedra of $[Fe(ent)]^{3-}$ (*left*) and $[Fe(D\text{-}ent)]^{3-}$ (*right*) with faces shown in blue and pink, respectively. Red spheres represent oxygen atoms at the vertices and the central iron atoms are shown as orange spheres. The individual angles averaged to obtain the twist angle α are indicated on the polyhedron of $[Fe(ent)]^{3-}$: $\alpha_1 = 36.5°$, $\alpha_2 = 37.1°$, $\alpha_3 = 36.3°$. Mean = 36.6°, standard error of the mean = 0.3°.

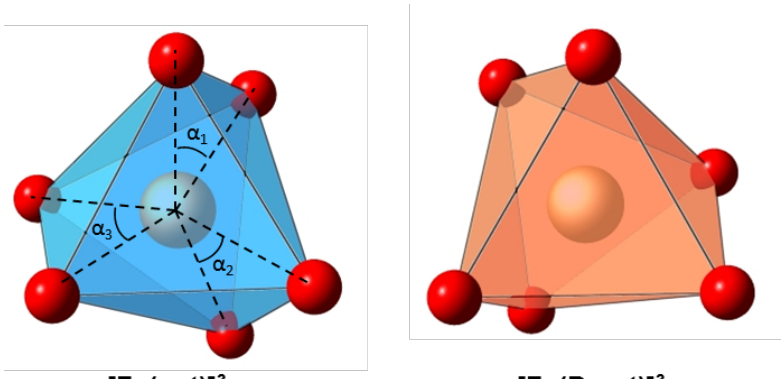

Figure S7. Solvent-filled voids viewed along the crystallographic *b* axis. Surfaces bounding the pockets of disordered solvent within a unit cell are shown in yellow. Modeled atoms are shown as balls and sticks. The void surfaces were generated with a 1.2 Å radius probe. Color code: Fe orange, O red, N blue, C black, As purple, H white.